Macromolecules
ARTICLE

Macromolecules **2010**, *43*, 8373–8378 **8373**
DOI: 10.1021/ma101272b

Structural Examination of Dissolved and Solid Helical Chiral Poly(trityl methacrylate) by VCD Spectroscopy

Christian Merten* and Andreas Hartwig

Fraunhofer Institute for Manufacturing Technology and Advanced Materials (IFAM), Bremen, Germany

Received June 8, 2010; Revised Manuscript Received September 13, 2010

ABSTRACT: The structures of the helical chiral polymer poly(trityl methacrylate), PTrMA, in solid state and in chloroform solution are compared by using vibrational circular dichroism spectroscopy. The differences between the spectra are discussed in detail based on band assignments and density functional theory calculations. Therefore, VA and VCD spectra of oligomers of PTrMA were calculated. It is shown that in solution as well as in solid state the helical structure is maintained. Furthermore, it was possible to determine the helical screw sense of the dextrorotary enantiomer (+)-PTrMA to be left-handed.

Introduction

Nowadays, chiral polymers are discussed for several applications. There is a special interest in chiral functional polymers, for instance polymers that can be used as switches or sensors whose current status can be detected by chiroptical methods. Further discussed applications also include optical data storage, catalysis, or chiral separation.[1−6]

Methods of characterization include, among others, X-ray analysis, atomic force microscopy (AFM), and nuclear magnetic resonance spectroscopy (NMR). The chirality of these polymers is in general characterized by electronic circular dichroism (ECD) spectroscopy.[7] This technique allows the detection of chiral superstructures like helical conformations and stuctural changes with the smallest amount of sample. A closer insight into the molecular conformation is unfortunately limited.

In the past years, vibrational circular dichroism (VCD) spectroscopy, the differential absorption of left- and right-circular polarized light during a vibrational transition, has grown to a powerful tool for the determination of absolute configuration of chiral molecules and aggregates in solution and the examination of the structure of biopolymers.[8−12] A VCD study is almost always a combination of experimental spectroscopy and density functional theoretical calculations of vibrational spectra. Hence, among others, the success of VCD spectroscopy is based on the increased computational power that became available in the past 10 years.

Furthermore, VCD spectroscopy offers the possibility to measure solid samples, e.g., solution-casted films of chiral polymers. These measurements may be difficult because of artifacts originating from linear dichroism and birefringance which occur as orientational effects during the measurement. However, when they are not too large, these effects can be easily eliminated.[13,14]

In the literature, there are only a few VCD studies concerning chiral synthetic polymers. First experimental works by McCann et al. dealt with menthol-substituted methacrylates and olefins.[15−17] More recently, Tang et al. reported the determination of the helical screw sense of a polyguanidine,[18,19] and Kawauchi et al. calculated the helical structure of st-PMMA with encapsulated fullerenes in the presence of a chiral alcohol.[20] The helix sense of a polyisocyanide has recently been determined by Hase et al.,[21] and the helical structure of an aromatic oligo(*m*-phenylurea) has been the focus of a work by Kudo et al.[22]

The potential to compare solid state structure of polymers and their structure in solution motivated the present study. The focus of this work is on poly(trityl methacrylate), which was reported to be the first optically active vinyl polymer whose chirality arises exclusively from its helical main chain conformation and not from any chiral substituent.[23−25] Poly(trityl methacrylate), short PTrMA, maintains its helical conformation by sterical repulsion of the bulky trityl groups which prevents the backbone from uncoiling. The actual origin of the chirality is the initiator/co-initiator of the anionic polymerization. Most commonly used is *n*-butyl lithium/(−)-sparteine, in which the butyl anion is the initiator. The lithium ion which is complexed by (−)-sparteine remains at the growing chain end and thus keeps the chain end in a chiral environment. A schematic illustration is given in Figure 1. Different types of initiator complexes have been applied to obtain chiral polymers with both positive and negative optical rotations. Also differently substituted monomers were used for the polymerization.

Several experiments and theoretical considerations were focused on the structure of poly(trityl methacrylate). Starting indirectly with the finding by Mislow that the phenyl rings in triphenylmethane have a propeller-like conformation,[26] the structure of PTrMA has been derived from the determination of its tacticity[27] and its stability in several solvents[28] as well as the conformation of the left-handed propeller conformation.[25,29] The first observation of the VCD of PTrMA has been reported in the thesis of J. McCann, but it has not been analyzed in further detail.[17]

In the present work, the vibrational absorption and circular dichroism spectra of a solution of poly(trityl methacrylate), more precisely the dextrorotary (+)-PTrMA, is compared with the spectra of solid samples. Afterward, the calculated VA and VCD spectra of (+)-PTrMA which are obtained from DFT calculations will be used to discuss the differences between the experimental spectra. It will be shown that these calculations can give further insight into the helical chiral structure of the polymer.

Materials and Methods

Materials. All chemicals were purchased from Sigma-Aldrich, Germany, except for d_1-chloroform which was obtained from Deutero GmbH, Germany. The chemicals were used without further purification.

*To whom correspondence should be addressed. E-mail: christian.merten@ifam.fraunhofer.de.

Published on Web 09/23/2010

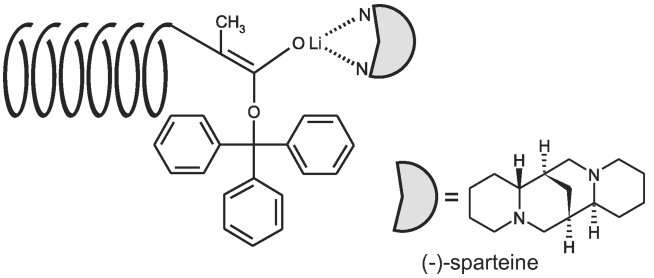

Figure 1. Chiral growing chain end of a PTrMA helix.[3]

Synthesis of (+)-Poly(trityl methacrylate). The synthesis was carried out according to the literature.[23] The monomer, trityl methacrylate, was synthesized by dissolving 5 g (17.8 mmol) of trityl chloride and 2.45 g (1.6 equiv) of freshly distilled methacrylic acid in 60 mL of dry THF and adding 4.2 mL (1.7 equiv) of Et_3N. After stirring for 2 h the reaction mixture was washed with $NaHCO_3$ and NaCl and recrystallized from hexane (72%, 4.2 g). The anionic polymerization with *n*-BuLi/(−)-sparteine was carried out with a monomer/initiator ratio of 20:1 in toluene. After 1.5 h of stirring at −40 °C the reaction mixture was warmed to room temperature, and the polymer was precipitated in methanol. $\alpha_D^{295} = +318°$ (c = 1.0, CH_2Cl_2).

VCD Measurements. The vibrational absorption and vibrational circular dichorism spectra were recorded using a Bruker Tensor 27 equipped with a PMA 50 module. VA and VCD spectra of PTrMA in solution were recorded in a mountable cell with KBr windows and a path length of 100 μm in the region from 1800 to 950 cm^{-1}. Baseline correction of these spectra was done by subtracting the spectrum of the solvent. The spectra of solid samples were recorded with KBr windows as substrate for solution-casted films.

Computational Details. All density functional theory calculations were performed using the 64 bit version of Gaussian 03[30] on a linux cluster with dual-core AMD Opteron processors (2.8 GHz) and 8 GB RAM per processor.

The level of theory for all calculations has been B3PW91/6-31G(d,p). The calculated VA and VCD spectra are presented by assigning a Lorentzian band shape with a half-width of 4 cm^{-1} to each fundamental vibration. The frequencies were scaled by a factor of 0.97 for a better comparison with the experimental data. For some calculations, the modredundant option was used to fix several internal coordinates.

Comment about the Choice of Units for the Presentation of the Spectra. For the measurements of (+)-PTrMA in solution, a nearly saturated solution in d_1-chloroform was used. The solid sample was obtained by solution casting of the residual solution onto a KBr window. The thickness of the solution-casted film was inhomogeneous, and thus, the VA and VCD spectra have to be compared in units of absorbance instead of molar absorptivity.

In order to compare the experimental VA and VCD spectra of (+)-PTrMA with spectra obtained from DFT calculations, the spectra were converted to molar absorptivity assuming a concentration of the saturated solution of ~10 mg/mL (equivalent to 30 mmol monomer/L). The calculated spectra of oligomers which will be discussed in the following sections were normalized to the number of monomers.

Results and Discussion

The vibrational absorption and circular dichroism spectra of (+)-poly(trityl methacrylate) have been recorded for a chloroform solution and in solid state. In Figure 2, the obtained VA and VCD spectra are compared. The solid state VCD spectra showed no orientational dependence. However, slightly different intensities of the VCD signals have been observed for different solid samples after normalization to the intensity of the carbonyl vibrational absorption band. They are assumed to originate from different crystallization rates or other reasons related to the preparation of the solid samples. Table 1 summarizes the band assignments which have been generated from a comparison of the VA spectrum of PTrMA with the one of PMMA[31−33] and with data from the literature.[34,35] The assignments are completed by results of the DFT calculations which will be discussed in the next section. It is important to note that the vibrational modes in the region from 1200 to 1100 cm^{-1} which are assigned to the wide variety of in-plane C−H bending vibrations of the phenyl rings are often strongly coupled with deformations of the helical backbone.

In the VA spectra of the solution and the solid samples significant differences between the intensities of several absorption bands can be observed. For instance, the absorption bands at 1471 and 1386 cm^{-1} which are assigned to the asymmetric and symmetric deformation vibration of the methyl group are much weaker for the solid state spectra. Further differences are observed in the

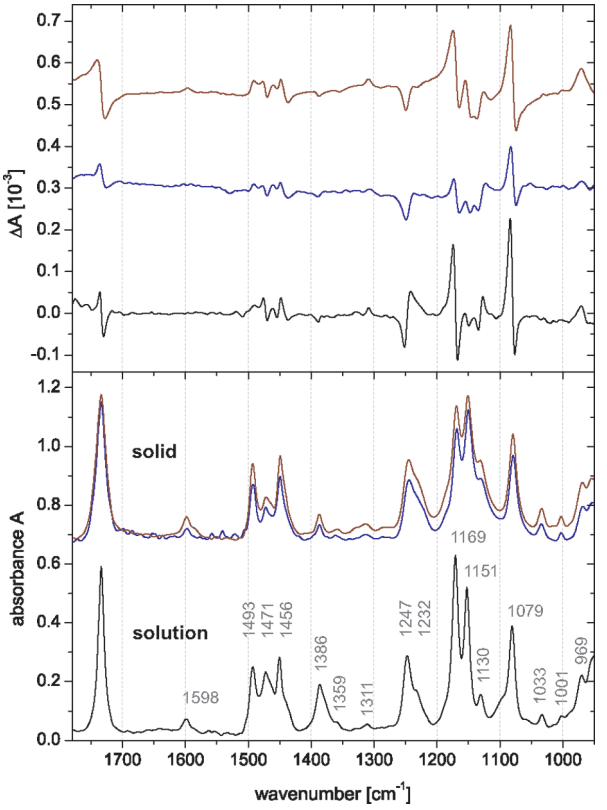

Figure 2. Experimental VA (bottom) and VCD spectra (top) of (+)-PTrMA in d_1-chloroform solution and in solid state.

Table 1. Band Assignments for the VA and VCD Spectra of PTrMA

wavenumber [cm^{-1}]	assigned group vibration
1732	C=O stretching vibration
1598	quadrant stretch of the phenyl ring
1493	semicircle stretch of the phenyl ring coupled with C−H in-plane bending
1471	CH_3 asymmetric deformation
1456	semicircle stretch of the phenyl ring coupled with C−H in-plane bending
1386	CH_3 symmetric deformation
1359	CH_2 wagging vibration
1311	CH_2 twisting vibration
1247	ester C−O stretching vibration coupled with deformation vibrations of the backbone
1232	in-plane C−H bending vibration
1169	in-plane C−H bending vibration
1151	in-plane C−H bending vibration
1130	in-plane C−H bending vibration
1079	in-plane C−H bending vibration
1033	in-plane C−H bending vibration

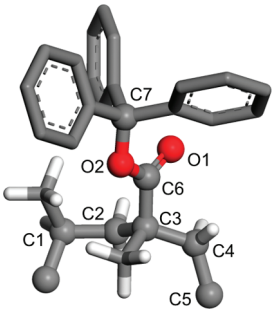

Figure 3. Atom numbering corresponding to the structural data of a fragment of PTrMA summarized in Table 2.

region 1200−1100 cm^{-1}. While the intensity of the 1169 cm^{-1} absorption band decreases relatively to the 1151 cm^{-1} band, the intensity of the 1130 cm^{-1} band of the in-plane C−H bending vibration increases. Additionally, there are differences between the VCD spectra as well. The VCD pattern in the region from 1500 to 1425 cm^{-1} changes due to the decrease of the intensity of the vibrational mode at 1471 cm^{-1}. In contrast, the absorption band at 1386 cm^{-1} has no affected counterpart neither in the solution spectrum nor in the spectra of the solid samples. More prominent changes seem to occur in the lower frequency region. The VCD couplet of the C−O vibration of the ester groups at 1247 cm^{-1} becomes an almost only negative VCD band. The 1200−1100 cm^{-1} region appears to vary dramatically especially when comparing the two different solid state spectra. However, in a one-to-one comparison of the VCD pattern of this region between the three VCD spectra it can be seen that the VCD signs do not change. Hence, the observed differences can be assumed to be only intensity variations.

It can be stated that only vibrational transitions involving movements of the helical backbone are affected by the transition from solution phase to solid state. Those of the trityl groups remain almost unchanged. Hence, it can be argued that the decrease of the available space for vibrational movements of the helical backbone is the main reason for the observed differences. Vibrational movements like the C=O stetching vibration are not affected since the stretch movement along the double bond is not restricted. In contrary, the deformation of the methyl group is strongly affected since it requires additional space. The vibrational absorption bands in region 1200−1100 cm^{-1} are due to in-plane C−H bending vibrations which are coupled with deformational movements of the helical backbone (C−C stretching as well as CH_2 deformations); hence, a weak influence on these VA and VCD bands can be observed.

There is one noticeable difference between the solution and the solid state spectra which is not easily explained by the decrease of space and mobility of the backbone: the VCD couplet of the ester group's C−O stretching vibration which seems to be a solely negative band in the solid state spectra. This vibration takes place at the key position between the helical backbone and the bulky trityl substituents. In order to get a closer insight into the nature of this vibration, and certainly also to determine the helical screw sense and the influence of the propeller conformation of the trityl groups on the VCD spectrum, density functional theory calculations have been carried out.

Typically, the calculations of VCD spectra and the closely related determinations of absolute configurations start with the theoretical evaluation of the conformational space of the molecule under investigation. For (+)-PTrMA, this investigation has been carried out by Cavallo et al. based on force field calculations.[36] The resulting helical structure is the initial point of the present spectra calculations.

In Figure 3, a fragment of the PTrMA helix model is shown to indicate the atom numbering of the torsion angles which define its

Table 2. Structural Data of the DFT Calculations of a PTrMA Helix Oligomer[a]

structure	τ_1	τ_2	χ_1	χ_2	β_1	β_2	β_3
ref 36	164.0	−75.0	−76.0	176.0	−160.0 (l)	178.0 (r)	−125.0 (l)
3mer	170.9	−78.4	−10.2	175.7	32.1 (l)	16.1 (l)	84.4 (l)
	171.7	−85.1	−20.5	168.5	31.9 (l)	25.5 (l)	82.2 (l)
			−30.9	162.4	26.6 (l)	174.4 (r)	95.5 (r)
3mer*	176.6	−78.9	−2.8	175.0	149.2 (r)	167.4 (r)	94.8 (r)
	172.7	−83.5	−49.7	174.8	151.2 (r)	174.9 (r)	90.5 (r)
			−45.4	−174.6	153.7 (r)	2.0 (l)	90.4 (r)
4mer	170.8	−76.9	−80.4	176.2	29.8 (l)	10.1 (l)	89.5 (l)
	168.8	−84.2	−15.8	169.9	29.8 (l)	23.7 (l)	86.2 (l)
	169.8	−82.5	−33.6	160.2	18.1 (l)	162.0 (r)	99.2 (r)
			−57.5	158.3	29.4 (l)	172.5 (r)	93.1 (r)
5mer	174.7	−74.2	−103.1	172.5	23.5 (l)	171.9 (r)	92.8 (r)
	163.8	−83.1	−21.9	169.2	30.3 (l)	25.9 (l)	84.3 (l)
	170.1	−84.5	−12.5	172.4	32.4 (l)	25.1 (l)	82.0 (l)
	170.2	−85.2	−39.5	156.3	12.9 (l)	154.9 (r)	109.7 (r)
			−56.1	158.9	28.2 (l)	169.3 (r)	94.3 (r)
6mer[b]	166.9	−84.9	−31.2	156.7	29.7 (l)	169.1 (r)	92.6 (r)
	177.8	−86.3	−31.7	162.8	101.8 (r)	24.6 (l)	162.7 (r)
	176.7	−87.4	−33.4	158.2	97.7 (r)	27.8 (l)	165.9 (r)
	167.1	−81.9	−18.4	172.0	29.2 (l)	79.2 (l)	39.3 (l)
	174.4	−77.2	−43.3	165.3	20.1 (l)	74.2 (l)	46.5 (l)
			−122.9	175.1	10.1 (l)	36.4 (l)	85.1 (l)
7mer[b]	167.3	−85.0	−53.4	159.7	34.2 (l)	88.5 (l)	171.4 (r)
	171.5	−86.7	−41.8	155.7	7.1 (l)	149.5 (r)	109.0 (r)
	176.5	−87.8	−37.1	158.9	17.5 (l)	152.8 (r)	106.7 (r)
	172.6	−87.6	−37.3	163.2	33.2 (l)	170.1 (r)	93.9 (r)
	163.0	−82.5	−8.4	−179.8	37.5 (l)	16.0 (l)	85.6 (l)
	175.6	−77.2	−45.1	167.7	23.1 (l)	49.4 (l)	71.3 (l)
			−113.4	174.6	87.4 (l)	1.5 (l)	34.2 (l)

[a] The angles are defined as follows: τ_1 = (C1−C2−C3−C4), τ_2 = (C2−C3−C4−C5), χ_1 = (C4−C3−C6−O1), and χ_2 = (C3−C6−O2−C7). The angles β are defined as O2−C7−C−C(H) into one of the rings. (l) and (r) indicate the orientation of each phenyl ring with respect to the propeller conformation of the trityl group. [b] Please note that the frequency analysis for the 6mer and the 7mer was not performed, and the structures are given as obtained from the geometry optimization.

structure. There are two backbone torsion angles τ_1 and τ_2 and two angles χ_1 and χ_2 determining the orientation of the ester group. The three angles β_1−β_3 adjust the propeller conformation of the phenyl rings. When β is in a range of $0° < \beta < 90°$, the phenyl ring is adjusted as in a left-handed propeller, and for $90° < \beta < 180°$ it is set as in a right-handed propeller. Using the values from the first line of Table 2, a left-handed 7_2 helix can be constructed whose fiber identity period comprises seven monomer units in two helix turns and whose trityl groups possesses a left-handed propeller structure.

Oligomers of PTrMA consisting of three to seven monomer units and methyl groups as terminating groups have been built up using these structural parameters. During the geometry optimizations all oligomers were allowed to fully relax without any constraints. Although all optimizations terminated normally, only the spectra calculations for the 3mer, 4mer, and 5mer completed successfully. The spectra calculations for larger oligomers broke down due to computer hardware limits. However, the characteristic torsion angles of all obtained structures are given in Table 2. As can be seen from the β angles, the initially mainly left-handed propeller evolved into partly right-handed structures. This is consistent with the earlier findings by Wang et al., who proposed that rotations along the phenyl−C bond (variation of the angles β) do not show a high energetical barrier.[29] Therefore, the calculations were rerun for a left-handed oligomer with a length of three monomer units and mainly right-handed propeller structures to evaluate the influence of the propeller conformation on the resulting spectra. This oligomer is denoted as 3mer* in Table 2.

In Figure 4, the successfully calculated VA and VCD spectra of the four oligomers (3mer to 5mer and 3mer*) are compared to the experimental spectra of the (+)-PTrMA solution. The calculated

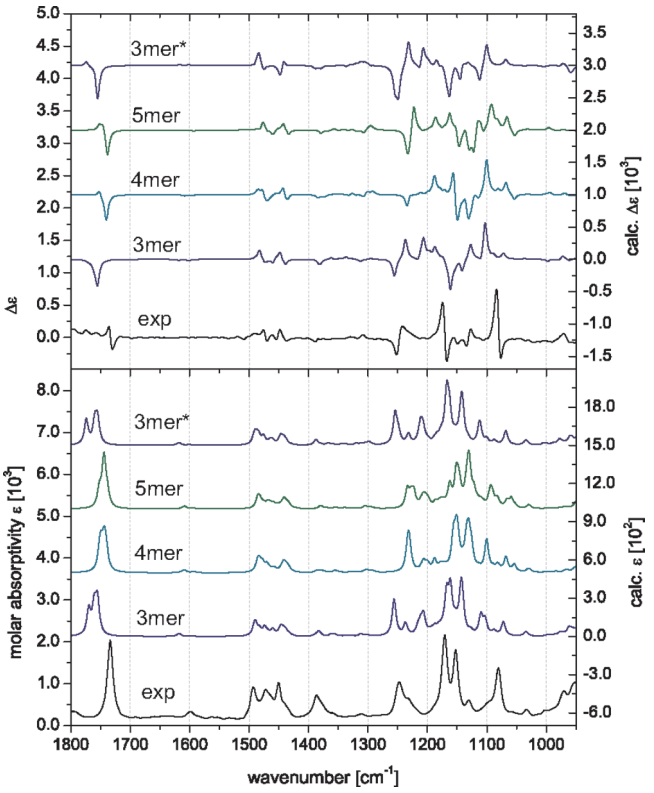

Figure 4. Comparison of the experimental VA and VCD of (+)-PTrMA with the calculated spectra of the full 3mer, 4mer, and 5mer as well as the 3mer*.

vibrational absorption spectra feature the characteristic experimental absorption pattern. Regarding the carbonyl vibration around 1730 cm^{-1} and the more characteristic part in the range from 1300 to 1100 cm^{-1}, it can be seen that the agreement becomes slightly better with increase of the oligomer length while the agreement in the region from 1500 to 1400 cm^{-1} is quite good for all fragments. For the theoretical VA spectra, the calculated absorption band for the carbonyl vibrations sharpens, and it can be observed that the frequencies of the vibrational modes forming the pattern between 1300 and 1200 cm^{-1} move closer together. This results in a broadening of the calculated pattern which becomes more and more similar to the experimental absorption band.

The deviations between the experimental and theoretical VCD spectra are more drastically. A similar evolution of the quality of the agreement between experimental and theoretical spectra like for the VA spectra can be deduced for the VCD spectra. For the shorter oligomers some VCD pattern qualitatively match the experimental ones while others seem completely different. For the 5mer, the agreement is already quite good since the significant experimental VCD pattern are reproduced.

This might be an effect of the geometry optimization. Since the oligomers were optimized without any constraints, especially the terminal carbonyl or ester groups had enough space to move out of the desired orientation. It can be expected that higher oligomers would show an even better agreement with the experiment.

It can be concluded from the present data that (+)-PTrMA adopts a left-handed helical structure. Furthermore, the conformation of the trityl propeller does not appear to have a strong influence on absorption bands assigned to backbone vibrations. This is deduced from the comparison of the spectra of the 3mer and the 3mer*. Although the propeller conformations are mostly left-handed for the 3mer and mostly right-handed for the 3mer*, only minor differences between the calculated VCD spectra can be observed.

In order to show that the main characteristics of the VCD spectrum of (+)-PTrMA which were assigned to the helical backbone occur independent of the trityl conformation and even independent of the type of substituent, further calculations have been carried out. Therefore, the initial structure model of the helical PTrMA as given in the first line of Table 2 was reduced to the structure of PMMA by simply substituting the trityl by methyl groups. To prevent the so-constructed helical structure from uncoiling during the geometry optimization due to a lack of the conformational anchor, the torsion angles were held under constraints. Both the geometry optimizations and the frequency calculations for the PMMA oligomers proceeded much faster which is not surprising since the runtime of calculations generally depends on the number of atoms. Because of the applied constraints, some of the calculations yielded negative frequencies; i.e., the geometries have not been optimized to an energetical minimum. Since the main focus of these calculations has been the backbone of PTrMA, this was accepted for the PMMA model structures.

In Figure 5, the calculated vibrational absorption and circular dichroism spectra of the PMMA oligomers are compared to the experimental spectra of (+)-PTrMA. It has to be noted that after passing the length of a full helix turn the spectra of the PMMA oligomers do not alter significantly. This has also been proposed for the PTrMA helix for which the spectra of such long oligomers could not be calculated. Furthermore, it can clearly be seen that the characteristic VCD pattern of the ester C=O and C−O vibrations at around 1730 and 1247 cm^{-1} are well reproduced by this simplified model structure. Hence, it can be concluded that the trityl groups do not influence the backbone vibrations.

After it has been shown that the helix sense could be determined by comparison of the calculated spectra with the experimental data, the discussion should be focused on the difference between the experimental spectra of the solution and solid samples again. The assumption that most of the differences between these spectra were due to the reduced free moving space for backbone vibrations is supported by all calculations. For instance, the calculations for PMMA underline that the spectral region of the in-plane C−H bending vibrations of PTrMA, mainly 1200−1100 cm^{-1}, is superimposed by backbone vibrations. Therewith the intensity deviations can be explained.

There is still no obvious explanation for the observed VCD pattern of the C−O vibration of the ester group at 1247 cm^{-1} for the solid sample. One effect could have been the more homogeneous arrangement of the trityl groups, i.e., that the trityl groups adopt a predominant propeller conformation in the solid state. Because of the unique chiral recognition ability of PTrMA,[37] there is no doubt that this highly ordered arrangement takes place in solid state. Nevertheless, since it has been shown that the conformation of the trityl group has no strong influence on the VCD of PTrMA, this effect might be excluded as reason for the change of the VCD pattern.

Another possible reason could be that some of the vibrational movements associated with the absorption band at 1247 cm^{-1} are weakend due to the transition from solution to solid state. Therefore, the modes predicted for this absorption band have been visually inspected in the GaussView program. Two different vibrational movements can be destinguished. On the one hand, there is a vibration for which only the ester carbon is moving and the quaternary carbon atom on the backbone and the oxygen atom connecting the trityl group are almost frozen and, on the other hand, a vibration for which all three atoms are in motion. It could be assumed that a movement of the oxygen atom might be energetically less favored in the solid state due to the immobility

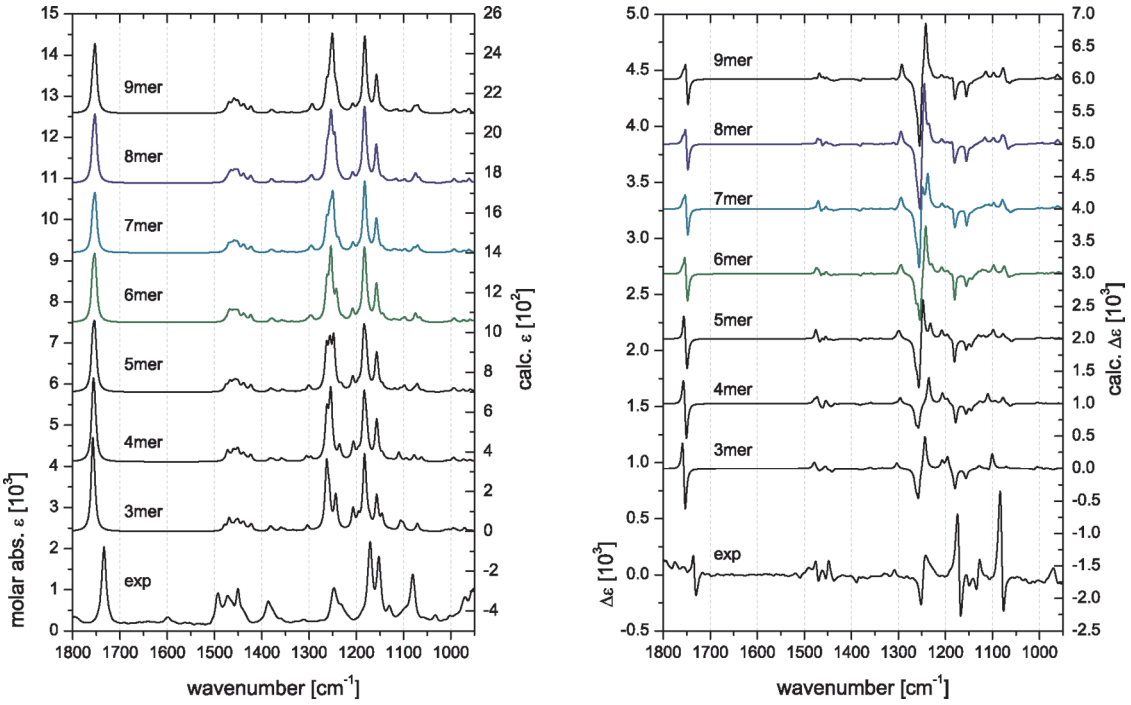

Figure 5. Comparison of the experimental VA and VCD spectra of (+)-PTrMA with the calculated spectra of oligomers of isotactic PMMA.

of the trityl groups. However, these two movements were found for both the positive and negative part of the couplet.

It is a matter of fact that the positive part of the couplet nearly vanished in the solid state spectra. Nevertheless, the reason for the decrease remains somehow speculative. Whether the intensity of the peak decreased or the VCD band of the neighboring vibrational mode at 1232 cm^{-1} changed its sign and therefore annihilated the positive part of the VCD band at 1247 cm^{-1} cannot be clarified.

Conclusion

The present work presents an experimental and theoretical investigation of the vibrational absorption and circular dichroism spectra of the helical chiral polymer (+)-poly(trityl methacrylate). Differences between the spectra of dissolved (+)-PTrMA and solid samples have been observed. After a detailed analysis of the band assignments, most of these differences could be explained. By comparison with calculated spectra, it was shown that the chiral propeller conformation has no significant influence on the VCD spectrum and that there are VCD pattern of backbone vibrations which are characteristic for the helical structure. Furthermore, it could be deduced from the results of the calculations that (+)-PTrMA possesses a left-handed helical structure. The characteristic VCD pattern which has been used to assign the handedness of the helical backbone was also obtained for a simplified PMMA model structure. Hence, it can be concluded that the determination of the screw sense can be carried out using smaller models as well which are faster and easier to calculate.

Bartus et al. compared the optical rotation of PTrMA in solution and suspension and concluded from the obtained very similar values that the structure of the polymer is identical in solution and solid state.[38] The present study supports these findings by comparing the infrared vibrational optical activity in a wide frequency range. It has also been observed that the intensities of the VCD spectra of PTrMA are about 1 order of magnitude higher compared to those of typical organic molecules. This increase can be attributed to the extended helical chiral structure of the polymer.

In future work further helical chiral polymers will be investigated. In particular, it will be of interest to evaluate whether there are characteristic VCD patterns for each class of polymer (e.g., bulky methacrylates, phenylacetylenes, etc.) which might be used to assign the predominant helix screw sense.

Acknowledgment. The authors thank Dr. Marc Amkreutz for fruitful discussions.

References and Notes

(1) Okamoto, Y.; Nakano, T. *Chem. Rev.* **1994**, *94*, 349–372.
(2) Green, M. M.; Peterson, N. C.; Sato, T.; Teramoto, A.; Cook, R.; Lifson, S. *Science* **1995**, *268*, 1860–1866.
(3) Nakano, T.; Okamoto, Y. *Chem. Rev.* **2001**, *101*, 4013–4038.
(4) Lam, J. W. Y.; Tang, B. Z. *Acc. Chem. Res.* **2005**, *38*, 745–754.
(5) Rudick, J. G.; Percec, V. *Acc. Chem. Res.* **2008**, *41*, 1641–1652.
(6) Yashima, E.; Maeda, K.; Furusho, Y. *Acc. Chem. Res.* **2008**, *41*, 1166–1180.
(7) Yashima, E. *Polym. J.* **2010**, *42*, 3–16.
(8) Freedman, T.; Cao, X.; Dukor, R. K.; Nafie, L. A. *Chirality* **2003**, *15*, 743–758.
(9) Urbanová, M.; Setnička, V.; Devlin, F.; Stephens, P. J. *J. Am. Chem. Soc.* **2005**, *128*, 6700–6711.
(10) Stephens, P. J.; Devlin, F. J.; Pan, J.-J. *Chirality* **2008**, *20*, 643–663.
(11) Keiderling, T. A. Vibrational Circular Dichroism Spectroscopy of Peptides and Proteins. In *Circular Dichroism. Principles and Applications*; Nakanishi, K., Berova, N., Woody, R. W., Eds.; VCH Publishers Inc.: Weinheim, 1994; pp 497−522.
(12) Keiderling, T. A. *Curr. Opin. Chem. Biol.* **2002**, *6*, 682–688.
(13) Buffeteau, T.; Lagugné-Labarthet, F.; Sourisseau, C. *Appl. Spectrosc.* **2005**, *59*, 732–745.
(14) Merten, C.; Kowalik, T.; Hartwig, A. *Appl. Spectrosc.* **2008**, *62*, 901–905.
(15) McCann, J.; Tsanokov, D.; Hu, N.; Liu, G.; Wieser, H. *J. Mol. Struct.* **1995**, *349*, 309–312.
(16) McCann, J. L.; Rauk, A.; Wieser, H. *J. Mol. Struct.* **1997**, *408*/*409*, 417–420.
(17) McCann, J. L. Ph.D. Thesis, The University of Calgary, 1998.
(18) Tang, H.-Z.; Novak, B. M.; He, J.; Polavarapu, P. L. *Angew. Chem., Int. Ed.* **2005**, *117*, 7464–7467.
(19) Tang, H.-Z.; Garland, E. R.; Novak, B. M.; He, J.; Polavarapu, P. L.; Sun, F. C.; Sheiko, S. S. *Macromolecules* **2007**, *40*, 3575–3580.

(20) Kawauchi, T.; Kumaki, J.; Kitaura, A.; Okoshi, K.; Kusanagi, H.; Kobayashi, K.; Sugai, T.; Shinohara, H.; Yashima, E. *Angew. Chem.* **2008**, *120*, 525–529.
(21) Hase, Y.; Nagai, K.; Iida, H.; Maeda, K.; Ochi, N.; Sawabe, K.; Sakajiri, K.; Okoshi, K.; Yashima, E. *J. Am. Chem. Soc.* **2009**, *131*, 10719–10732.
(22) Kudo, M.; Hanashima, T.; Muranaka, A.; Sato, H.; anbd Isao Azumaya, M. U.; Hirano, T.; Kagechika, H.; Tanatani, A. *J. Org. Chem.* **2009**, *74*, 8154–8163.
(23) Okamoto, Y.; Suzuki, K.; Ohta, K.; Hatada, K.; Yuki, H. *J. Am. Chem. Soc.* **1979**, *101*, 4763–4765.
(24) Okamoto, Y.; Suzuki, K.; Yuki, H. *J. Polym. Sci.* **1980**, *18*, 3043–3051.
(25) Okamoto, Y.; Honda, S.; Yashima, E.; Yuki, H. *Chem. Lett.* **1983**, 1221–1224.
(26) Mislow, K. *Acc. Chem. Res.* **1976**, *9*, 26–33.
(27) Yuki, H.; Hatada, K.; Niinomi, T.; Kikuchi, Y. *Polym. J.* **1970**, *1*, 36–45.
(28) Hosoda, M.; Schönhausen, U.; Pino, P. *Makromol. Chem.* **1993**, *194*, 223–232.
(29) Wang, Y.; Ding, M.; Wang, F. *Makromol. Chem.* **1991**, *192*, 1769–1775.
(30) Frisch, M. J.; et al. *Gaussian 03, Revision E.01*; Gaussian, Inc.: Wallingford, CT, 2004.
(31) Berghmans, H.; Smets, G. *Makromol. Chem.* **1968**, *115*, 187–197.
(32) Dybal, J.; Krimm, S. *Macromolecules* **1990**, *23*, 1301–1308.
(33) Lipschitz, I. *Polym.-Plast. Technol. Eng.* **1982**, *19*, 53–106.
(34) Eide, O.; Ystenes, M.; Støvneng, J.; Eilertsen, J. *Vib. Spectrosc.* **2007**, *43*, 210–216.
(35) Weston, R. E.; Tsukamoto, A.; Lichtin, N. N. *Spectrochim. Acta* **1966**, *22*, 433–453.
(36) Cavallo, L.; Corradini, P.; Vacatello, M. *Polym. Commun.* **1989**, *30*, 236–238.
(37) Okamoto, Y.; Hatada, K. *J. Liq. Chromatogr.* **1986**, *9*, 369–384.
(38) Bartus, J.; Vogl, O. *Polym. Bull* **1992**, *28*, 203–210.